Journal of Molecular Liquids 344 (2021) 117761

Contents lists available at ScienceDirect

Journal of Molecular Liquids

journal homepage: www.elsevier.com/locate/molliq

Cytotoxic effect, spectroscopy, DFT, enzyme inhibition, and moleculer docking studies of some novel mesitylaminopropanols: Antidiabetic and anticholinergics and anticancer potentials

Ali N. Khalilov [a,b,*], Burak Tüzün [c,*], Parham Taslimi [d,e], Ayca Tas [f], Zuhal Tuncbilek [g], Nese Keklikcioglu Cakmak [h]

[a] Organic Chemistry Department, Baku State University, Z. Khalilov Str. 23, Az 1148 Baku, Azerbaijan
[b] "Composite Materials" Scientific Research Center, Azerbaijan State Economic University (UNEC), H. Aliyev Str. 135, Az 1063 Baku, Azerbaijan
[c] Plant and Animal Production Department, Technical Sciences Vocational School of Sivas, Sivas Cumhuriyet University, Sivas, Turkey
[d] Department of Biotechnology, Faculty of Science, Bartin University, 74100 Bartin, Turkey
[e] Department of Chemistry, Faculty of Science, Istinye University, Istanbul, Turkey
[f] Department of Nutrition and Diet, Faculty of Health Sciences, Sivas Cumhuriyet University, Sivas, Turkey
[g] Department of Biochemistry, Faculty of Medicine, Sivas Cumhuriyet University, Sivas, Turkey
[h] Department of Chemical Engineering, Faculty of Engineering, Sivas Cumhuriyet University, Sivas, 58140, Turkey

ARTICLE INFO

Article history:
Received 20 July 2021
Revised 30 September 2021
Accepted 2 October 2021
Available online 09 October 2021

Keywords:
β-Amino alcohols
MTT
DFT
Molecular docking
Enzyme
Cell culture

ABSTRACT

β-Amino alcohols (2–4) used in this study were re-synthesized in accordance with our previous study. All compounds were characterized by the combination of NMR, UV–Vis, IR experimental and theoretical spectral data. Then, the cytotoxic activity studies of the molecules on SH-SY5Y and L-929 cell lines showed that compound 2 has the highest activity on SH-SY5Y cells. Afterwards, the inhibition properties of these derivatives were tested toward acetylcholinesterase (AChE) and α-Glycosidase (α-Gly) enzymes. The studied molecules were optimized on B3LYP, HF, M062X level 3–21 g, 6–31 g, and SDD basis sets. Molecular docking calculations were made to determine the biological activity values of the amino alcohols against the enzymes. Finally, the drug properties of molecules were investigated by ADME/T analysis.

1. Introduction

The β-amino alcohol units are the predominant structural motif in a range of natural and synthetic biologically active molecules [1]. They are one of the most significant molecules in medicinal chemistry. Amino alcohol derivatives are currently being studied for their antimicrobial, antifungal activities, antimalarial activity, cytotoxicity activity against cancer cells, as β-adrenergic blocking agents, enzyme inhibitors and etc. [2–6]. They also used as an effective chiral building block and chiral catalyst or ligand in organic synthesis [7–8]. In accordance with the high value of amino alcohols, various synthetic methods have been reviewed in the literature [9–11].

Neuroblastoma (NB) is the most common extracranial pediatric solid tumor that occurs in the sympathetic nervous system. NB, originates from the neural crest, and although it is mostly seen in the adrenal glands, it is seen in areas such as the paraspinal ganglion, thorax, neck, and pelvis [12]. NB constitutes 8–10% of all childhood cancers and is responsible for 15% of deaths due to pediatric tumors [13]. The 3-year survival rate of children in the high-risk group is approximately 20% [14]. Chemotherapy is among the appropriate strategies used for the treatment of NB in case of high risk of metastasis or tumor recurrence and after surgical tumor resection [15,16]. Anthracycline antibiotics (doxorubicin), camptothecins (topotecan/irinotecan), alkylating agents (cyclophosphamide/ifosfamide), epipodophylotoxins (etoposide), vinca alkyloids (vincristine) and heavy metals (cisplatin) are administered within the scope of chemotherapy [17,18]. Studies

* Corresponding authors at: Organic Chemistry Department, Baku State University, Z. Khalilov Str. 23, Az 1148 Baku, Azerbaijan (A.N. Khalilov).
E-mail addresses: xalilov_a@yahoo.com (A.N. Khalilov), theburaktuzun@yahoo.com.tr (B. Tüzün).

https://doi.org/10.1016/j.molliq.2021.117761
0167-7322/

on new drugs continue due to the heterogeneity of NB, its resistance to drugs and the high toxicity of the drugs administered [19].

Alzheimer's disease (AD) is related to defect in the level of substrates of cholinergic enzymes and the inhibition of acetylcholine esterase (AChE) that catalyzes acetylcholine (ACh) neurotransmitter is one of the treatment approaches for AD according to the cholinergic theory [20,21]. Diabetes is one of the serious diseases globally with many complications. One of therapeutic approaches for non-insulin-dependent diabetes mellitus (DM) is the inhibition of carbohydrate degradative enzymes that breakdown glycosidic bonds in polysaccharide molecules [22,23].

In this study, With theoretical calculations, important information about the chemical and biological activities of molecules is obtained [24,25]. Chemical properties of molecules were investigated by quantum chemical parameters obtained by program. However, experimental and theoretical NMR, IR, and UV–vis spectrum of the molecules were obtained. The obtained experimental and theoretical spectrum were compared with each other. On the other hand, molecular docking calculations were made to compare the activities of molecules against enzyme proteins. Finally, the biological activities of the molecules were compared by ADME/T analysis and it was tried to predict human metabolism effect and response. We aimed to determine the cytotoxicity of the newly synthesized **2**, **3** and **4** drugs (Fig. 1.) by applying them to the SH-SY5Y neuroblastoma cell line and the L-929 healthy mouse fibroblast cell line.

2. Material and methods

2.1. Experimental section

2.1.1. General comments

Mp's were determined using open glass capillaries on a Stuart SMP30 melting point apparatus and are uncorrected. All the chemicals were synthesized or obtained from commercial sources (Merck) and used as received. ^{1}H and ^{13}C NMR spectra were recorded at room temperature on a Bruker Avance II + 300 (UltraShield^{TM} Magnet) spectrometer operating at 300.130 and 75.468 MHz for proton and carbon-13, respectively, in DMSO d_6 and CCl_4 solutions with TMS as internal standards. Chemical shifts are reported in δ (ppm).

2.1.2. General procedure for the synthesis of compounds (**2–4**)

In pressure relief reaction vials to the vigorously stirred suspension of 10 mmol 1-chloro-3-mesitylpropan-2-ol **1** in 20 mL water was added 30 mmol of amine and heated in 90 °C for 4–24 h until the reaction mixture become homogeneous. Then the reaction mixture was cooled down. Reaction products was precipitated from reaction mixture as a white solid (or as a yellow oil **3**), collected by filtration and washed with distilled water. Crude products were recrystallized from cold CCl4 solution, the oil **3** was purified by column chromatography over silica gel and eluted with hexane: 2-propanol (60:40, v/v).

2.2. In vitro assay for cytotoxicity activity (MTT assay)

Cytotoxic activity of compound **2**, **3** and **4** on SH-SY5Y cell line and L-929 cell line was analyzed using 3-[4,5-dimethylthiazol-2-yl]-2,5 diphenyl tetrazolium bromide (MTT) method. DMEM (Dulbecco's Modified Eagle Medium) medium supplemented with 10% fetal bovine serum (FBS), 1% penicillin–streptomycin and 1% L-glutamine was used for cell lines. Cell lines were incubated at 37 °C, 95% humidity and 5% CO_2. Cells ($1x10^5$/well) were seeded in 96-well plates, and after 24 h of growth, the indicated compounds were applied to the cells at concentrations of 1, 10, 25, 50, 70, 80, 90 and 100 μM in a volume of 1 μL. Cells were exposed to these drugs for 24, 48 and 72 h of incubation. At the end of these periods, MTT was measured. Therefore, 10 μL MTT prepared with phosphate buffer saline at a concentration of 5 mg/ml was added to each well and incubated for 3 h at 37 °C in an environment containing 5% CO_2. After the medium containing MTT was aspirated, dimethyl sulfoxide (DMSO) was used to dissolve the formazan crystals. 100 μL DMSO was added and incubated for 15 min at room temperature on the shaker and absorbance values were read with a microplate reader UV spectrophotometer at 570 nm wavelength. These measurements were made in 3 repetitions for each sample and repeated in at least three different passage numbers. IC_{50} values were calculated using GraphPad Prism and graphs were generated. The obtained data were compared.

2.3. Cell morphology

SH-SY5Y and L-929 cells (5x105 cells/well) were plated into the plate. 1 μM of Compound **2**, **3** and **4** was added to each of the cells. Changes in cell morphology were observed on the cell imaging device (ZEISS Axio Vert.A1) at 20X magnification. The groups were compared with each other.

2.4. Statistical analysis

SPSS (Statistical Package for Social Sciences, ver: 25.0) program was used to evaluate the data in the study. All experiments were run in triplicate and the results expressed as mean ± SEM. The data were analyzed using one-way ANOVA and differences were considered significant ($^{*}p < 0.05$, $^{**}p < 0.01$ and $^{**}p < 0.0001$).

2.5. In silico calculation

2.5.1. Gaussian calculation

With theoretical calculations, it has become possible to have a lot of information about the chemical and biological activities of molecules before experimental procedures. Many calculation programs are used for these theoretical calculations. The programs are GaussView 5.0.8 and Gaussian09 AS64L-G09RevD.01 package [26,27] were used in this study. It was calculated using the Hartree–Fock (HF) [28] (Vautherin & Brink, 1972), Becke, 3-

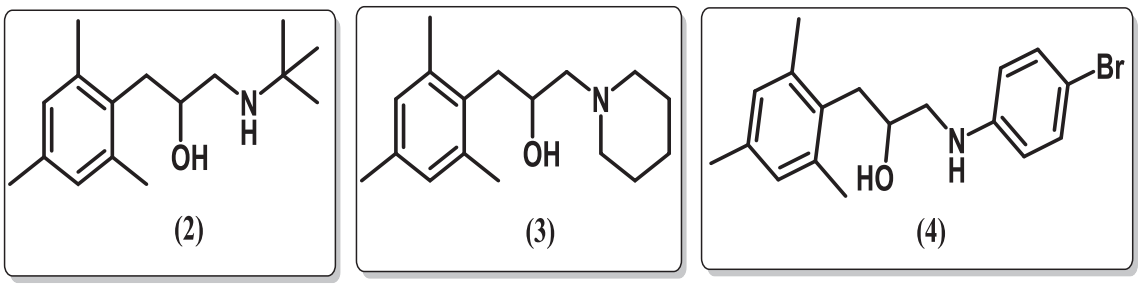

Fig. 1. Structures of β-amino alcohols 2–4.

parameter, Lee–Yang–Parr (B3LYP) [29–31] (Becke, 1993; Stephens et al., 1994; Wiberg, 2004), M06–2X [32] (Hohenstein et al., 2008) level with 3–21 g, 6–31 g and SDD basis set in these calculations. As a result of theoretical calculations, many quantum chemical parameters are obtained. Highest Occupied Molecular Orbital (HOMO) and Lowest Unoccupied Molecular Orbital (LUMO) values are the most significant among the parameters. Quantum chemical parameters such as E_{HOMO}, E_{LUMO}, ΔE (HOMO-LUMO energy gap), chemical hardness (η), chemical potential (μ), nucleophilicity (ε), electronegativity (χ), electrophilicity (ω), global softness (σ) and proton affinity (PA) are obtained from the quantum chemical calculations [33–35].

2.5.2. Molecular docking calculation

Molecular docking calculations have been made to examine the biological activity of molecules against proteins. For these calculations, calculations are made by the Maestro Molecular modeling platform (version 12.2) by Schrödinger [36]. These calculations consist of many processes. This process involves the calculation of both proteins and molecules. Firstly, active sites of proteins were determined by using the protein preparation module [37] for porteins. As a result, the proteins in the active region were given freedom to interact with them. the LigPrep module [38] was then used for the molecules. This module finds all conformers of the molecules and prepares them for interaction with proteins. In the next step, the Glide ligand docking module [39] is used for the interaction of molecules with proteins. In these calculations, the preparation and interaction of molecules and proteins were calculated using the OPLS3e method. As a result of these calculations, molecules have been interacted with proteins. The biological activities of molecules were compared against proteins. Then, ADME/T analysis (absorption, distribution, metabolism, excretion and toxicity) was performed to investigate the drug properties of these molecules. The Qik-prop module [40] of the Schrödinger software was used for this analysis.

2.6. Enzymes assays

The ChE inhibitory activities of the title compounds against AChE were determined by Ellman's method [41]. In this assay, AChE from electric eel (*Electrophorus electricus*) was used. α-Glucosidase inhibitory activity of novel derivatives was determined according to the reported method by Tao et al. [42].

3. Results and discussion

β-Amino alcohols were re-synthesized according to the literature [12]. The reaction scheme is illustrated in Scheme 1.

3.1. Cancer cells

The cytotoxic activities of the synthesized Compound 2, Compound 3 and Compound 4 drugs were evaluated on the SH-SY5Y (Figs. 2–4) human neuroblastoma cancer cell line and the L-929 healthy mouse fibroblast cell line (Figs. 5–7) (Table 1). Percentage of viability of control group and treatment group cells was calculated and compared with each other. According to the data obtained from the cellular cytotoxicity test, it has been shown that the compounds are effective on cells. When the IC_{50} values were compared, it was found that the compounds were more effective in the SH-SY5Y cell line than the L-929 cell line. SH-SY5Y cancer cells were able to show cytotoxicity at lower doses of the compounds synthesized than the L-929 healthy cells.

The results showed that the cytotoxicity of the compounds on SH-SY5Y and L-929 cells was at 72 h most active. Among the compounds applied to SH-SY5Y cancer cells, the most active cytotoxic one was evaluated as compound 2; then compound 3 and compound 4 were found, respectively. Compound 2 showed the highest activity at 72 h with an IC_{50} concentration of 4,43 ± 0.34 μM on SH-SY5Y cells compared to other compounds. The IC_{50} concentration required for the L-929 cell line of Compound 2 is 100 μM for 24 h, 48,48 ± 1.02 μM for 48 h and 42,06 ± 0.35 μM for 72 h, respectively. Compound 2 showed less cytotoxicity than other compounds.

The cytotoxicity of Compound 4 was observed in SH-SY5Y cells with an IC_{50} concentration of 7,88 ± 2.11 μM in the most active 72 h. Compound 2 showed lower activity in L-929 cells with an IC_{50} concentration of 42,06 ± 0,35 μM.

After applying 10 μM Compound 2, Compound 3 and Compound 4 compounds to SH-SY5Y and L-929 cells, morphological analyzes were performed (Fig. 8). According to the SH-SY5Y control group, a significant change in the morphology of the cells given Compound 2, Compound 3 and Compound 4 was detected. When compared to healthy L-929 cells with SH-SY5Y cells treated with Compound 2, Compound 3 and Compound 4, no morphological changes were observed in L929 cells of all three drugs. As a result, it was determined that all three compounds were active in SH-SY5Y neuroblastoma cells. When the three compounds applied to SH-SY5Y cells are compared, we can say that Compound 2 and Compound 4 have more effect.

In a previous study, chemotherapy drugs such as docetaxel and paclitaxel, which are widely used in various cancer types, were applied to the SY-SH5Y neuroblastoma cell line. It has been determined that docetaxel shows a high rate of cytotoxicity with IC_{50} values in the range of 2–11 μM [43]. In our study, we determined the IC_{50} value of Compound 2 and Compound 4 after 24 h and 48 h incubation in the range of 4–11 μM. Therefore, when the *in vivo* studies and mechanisms of action of the drugs we synthesized are completed, docetaxel may be an alternative drug candidate.

3.2. Theoretical calculations

With theoretical calculations, important information about the chemical and biological activities of molecules is obtained [44]. Many quantum chemical parameters are obtained from quantum chemical calculations. By comparing the numerical values of these

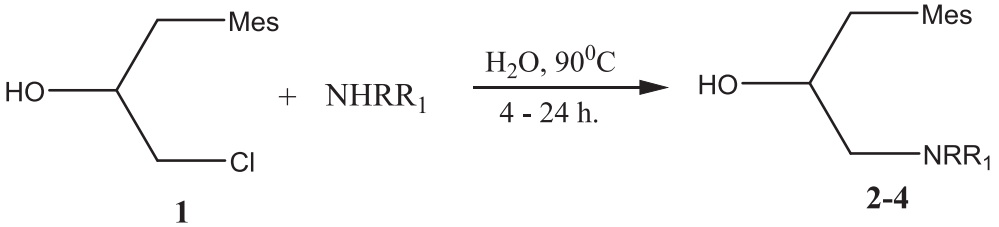

$NHRR_1$ = *tert*-butylamine (**2**), piperidine (**3**), 4-bromoaniline (**4**)

Scheme 1. Resynthesize of β-amino alcohols (**2-4**) used in this study.

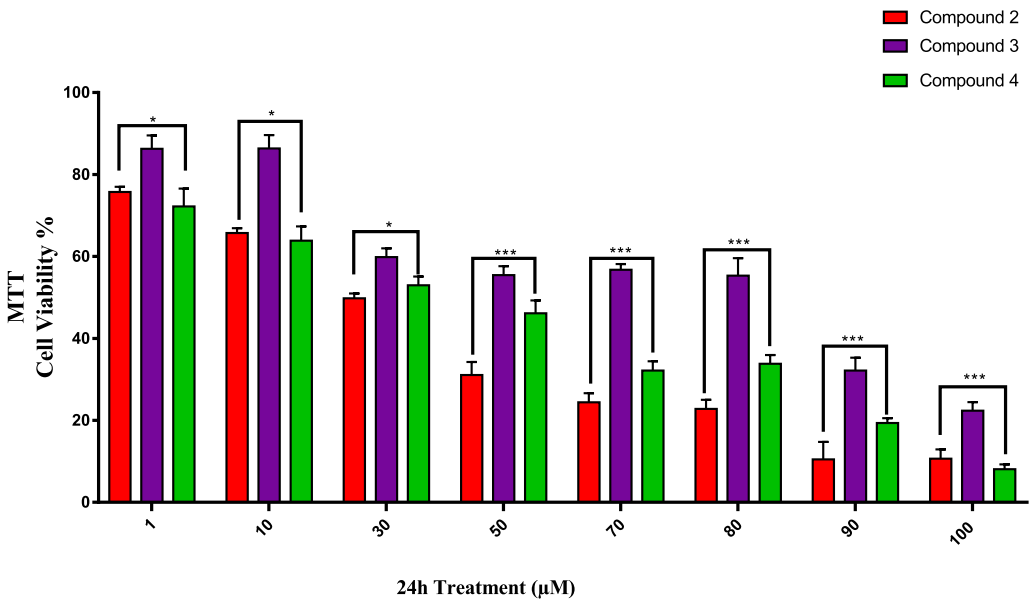

Fig. 2. Cytotoxicity study of Compound 2, 3 and 4 on SH-SY5Y cells. The treatment of SH-SY5Y cells was performed with these groups for a period of 24 h at concentrations varying between 1 and 100 μM. Every bar represents the mean + SEM of three separate tests (***$p < 0.0001$ and *$p < 0.01$).

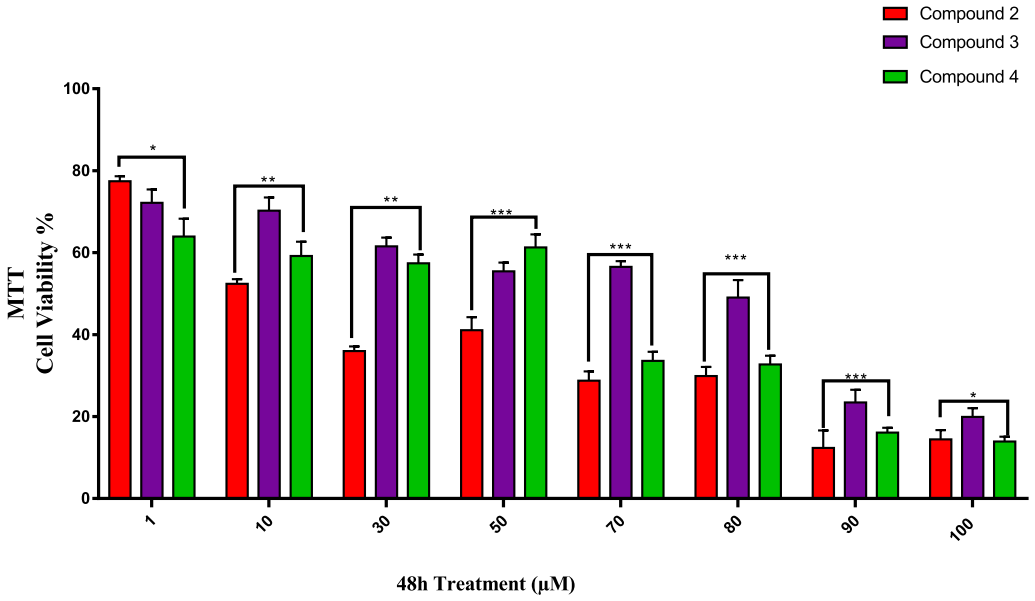

Fig. 3. Cytotoxicity study of Compound 2, 3 and 4 on SH-SY5Y cells. The treatment of SH-SY5Y cells was performed with these groups for a period of 48 h at concentrations varying between 1 and 100 μM. Every bar represents the mean + SEM of three separate tests (***$p < 0.0001$, **$p < 0.001$ and *$p < 0.01$).

quantum chemical parameters, it is possible to compare the chemical activity of the molecules. Among the parameters used for this comparison, the most used and known are HOMO and LUMO, these parameters are used to explain intermolecular interactions. HOMO is Highest Occupied Molecular Orbital and LUMO is Lowest Unoccupied Molecular Orbital [45]. The HOMO parameter of the molecules shows the molecule's ability to donate electrons [46]. The molecule with the most positive energy values of the electrons in the HOMO orbitals gives this electron more easily and quickly [47]. As a result, the chemical activity of this molecule is highest. However, the LUMO energy value of the molecules is very important for their chemical activity. The molecule with the lowest energy value of the LUMO orbitals of the molecules is easier and faster to accept electrons into these orbitals [48]. That is, it shows the easier and faster acceptance of electrons by molecules. These two parameters provide important information about the chemical activities of the molecules. Although other parameters are important for the chemical activities of the molecules, they are calculated from the HOMO and LUMO energy values. More detailed information for these parameters is given in previous studies. All calculated parameters of compounds 2, 3, and 4 are given in Table 2.

Although many parameters are obtained from the calculations, few of them have a visual representation. In which, in Fig. 9, first optimized versions of the molecules are given. Afterwards, the atoms on which the HOMO and LUMO orbitals of the molecules are concentrated, are given. Finally, molecular electrostatic potential (ESP) of the molecules is given, which gives information about the electron density in the molecule. In the ESP views of the molecules, the dark red regions are the regions with the highest electron

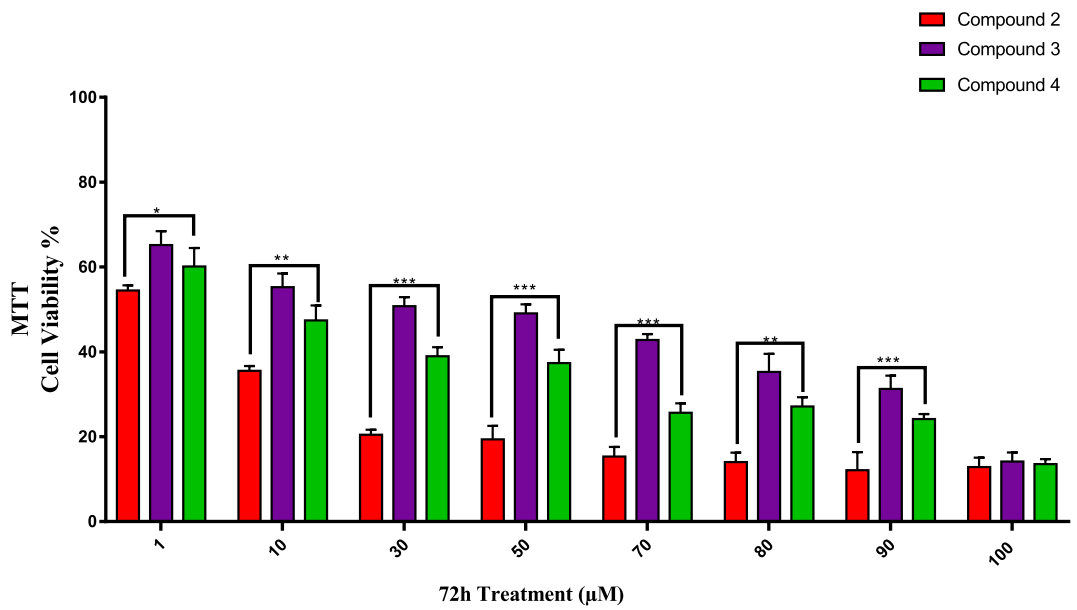

Fig. 4. Cytotoxicity study of Compound 2, 3 and 4 on SH-SY5Y cells. The treatment of SH-SY5Y cells was performed with these groups for a period of 72 h at concentrations varying between 1 and 100 μM. Every bar represents the mean + SEM of three separate tests (***$p < 0.0001$, **$p < 0.001$ and *$p < 0.01$).

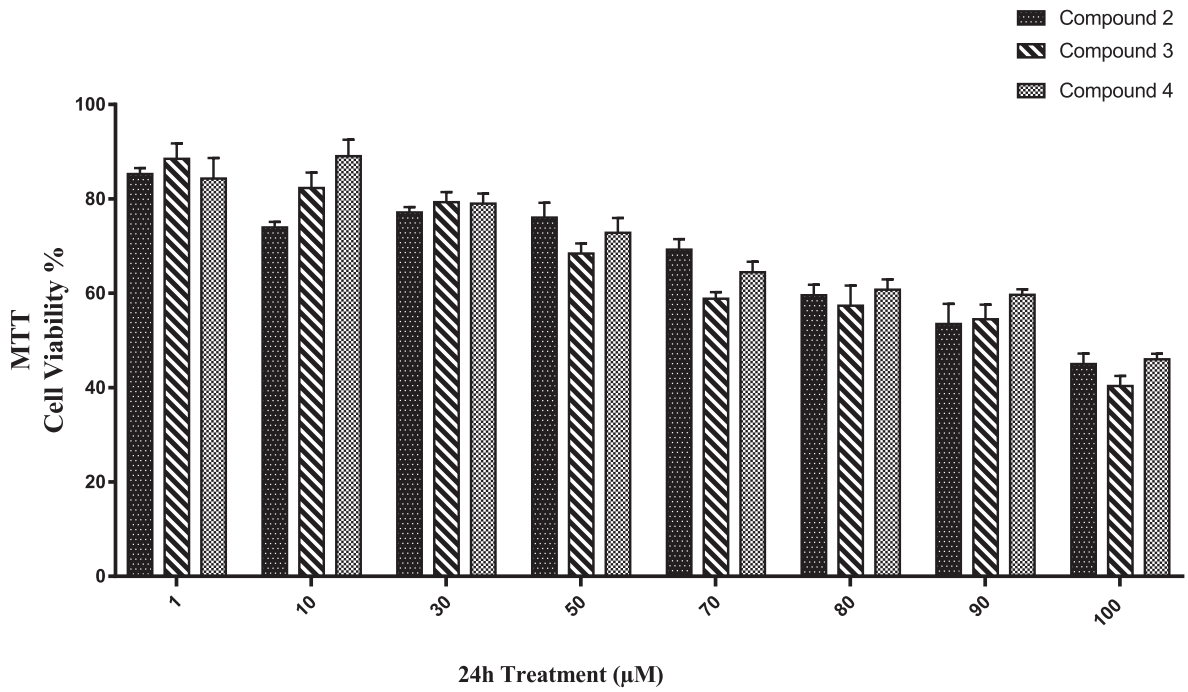

Fig. 5. Cytotoxicity study of Compound 2, 3 and 4 on L-929 cells. L-929 cells were treated with these drugs for 24 h in a concentration range of 1 to 100 μM. Represents the mean ± SEM of three separate experiments.

density. On the other hand, the light blue regions are the regions with the least electron density. Other fields are shown in green [49].

For the characterization of the molecules studied, NMR, IR, and UV–vis spectra of the molecules were obtained and compared both experimentally and theoretically.

3.2.1. Nuclear magnetic resonance analysis

In this characterization, first NMR analysis was performed. NMR (Nuclear Magnetic Resonance) analysis is one of the three most important methods used to determine the structure of molecules. This analysis is based on measuring the absorption of all the atoms in the molecule of the beam sent to the molecule as a result of the absorption of electromagnetic radiation in the radio frequency range. In experimental and theoretical studies, NMR chemical shift values of carbon (^{13}C) and hydrogen (^{1}H) atoms were calculated. In theoretical calculations, numerical values were found using the Gauge-Independent Atomic Orbital (GIAO) method [50]. NMR analysis was done at room temperature on a Bruker Avance II + 300 (UltraShieldTM Magnet) spectrometer operating at 300.130 and 75.468 MHz for proton and carbon-13, respectively. Experimental and theoretical pictures of NMR spectra are given

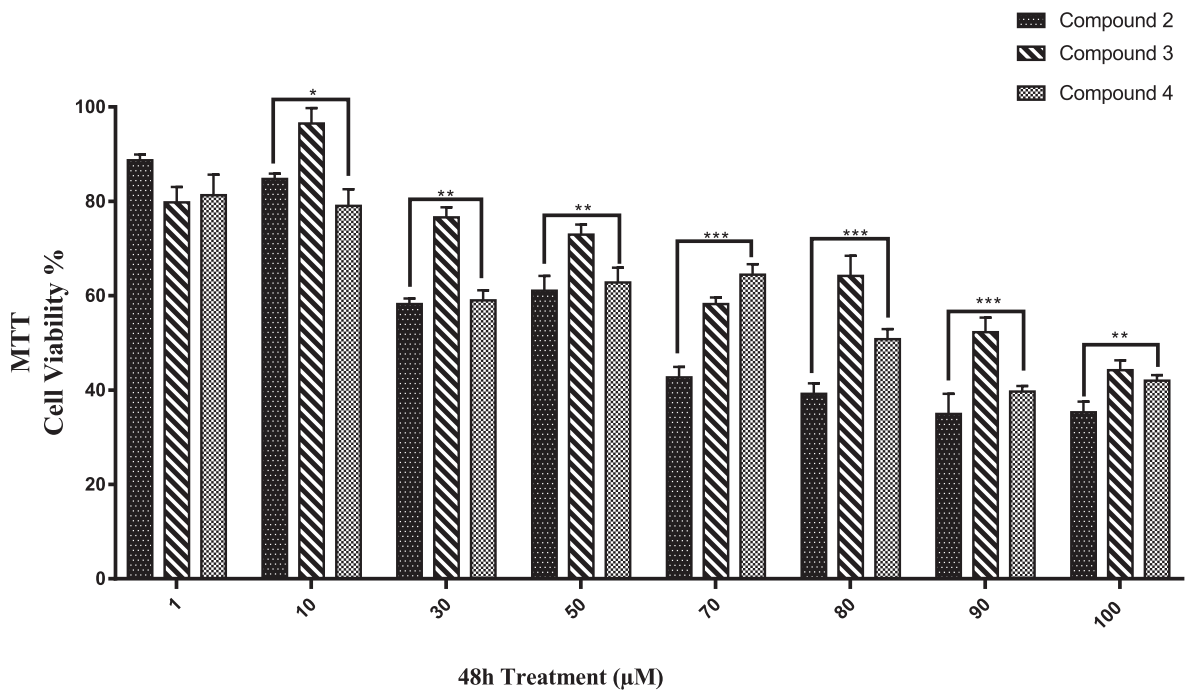

Fig. 6. Cytotoxicity study of Compound 2, 3 and 4 on L-929 cells. L-929 cells were treated with these drugs for 48 h in a concentration range of 1 to 100 μM. Represents the mean ± SEM of three separate experiments. (***$p < 0.0001$, **$p < 0.001$ and *$p < 0.01$).

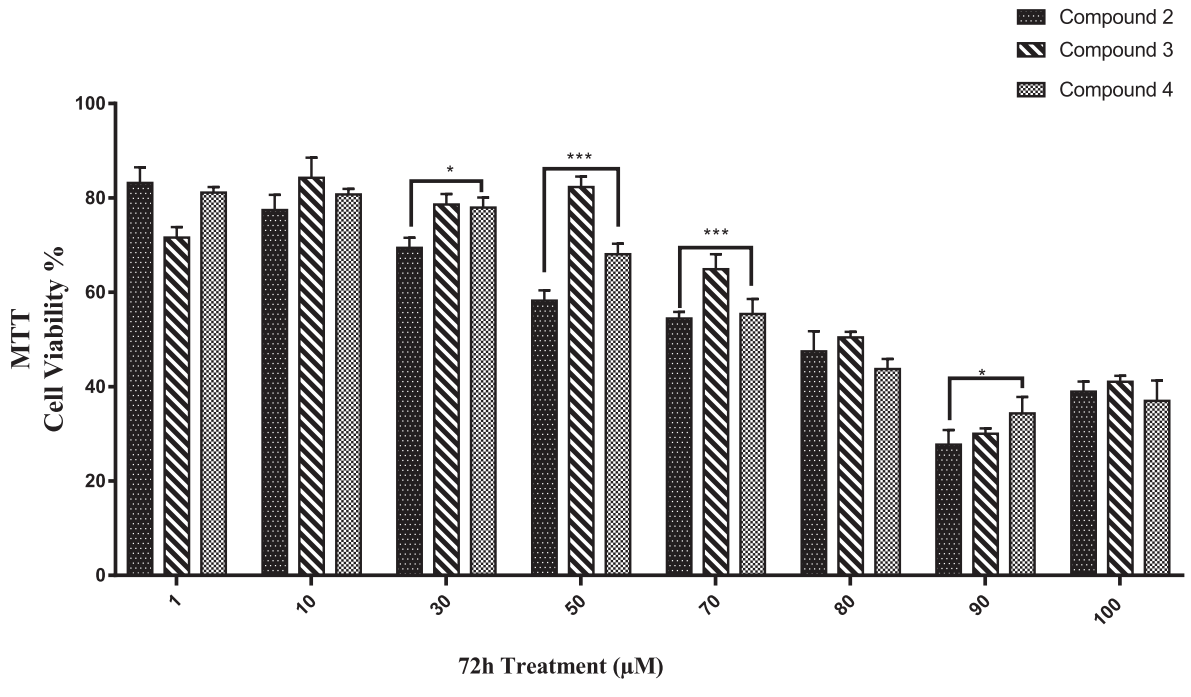

Fig. 7. Cytotoxicity study of Compound 2, 3 and 4 on L-929 cells. L-929 cells were treated with these drugs for 72 h in a concentration range of 1 to 100 μM. Represents the mean ± SEM of three separate experiments. (***$p < 0.0001$ and *$p < 0.01$).

Table 1
Comparing IC_{50} values between Compound 2, 3 and 4 on SH-SY5Y and L929 cell lines following incubation for 24 h, 48 h, and 72 h.

Drugs	SH-SY5Y IC_{50} (μM ± SD*)			L929		
	24 h	48 h	72 h	24 h	48 h	72 h
Compound 2	16.32 ± 1.02	7.05 ± 1.98	4.43 ± 0.34	≥100	48.48 ± 1.02	42.06 ± 0.35
Compound 3	83.68 ± 2.67	53.16 ± 1.56	48.89 ± 2.09	≥100	81.19 ± 2.17	51.63 ± 3.03
Compound 4	11.71 ± 3.34	8.93 ± 1.44	7.88 ± 2.11	≥100	56.05 ± 1.98	47.00 ± 1.36

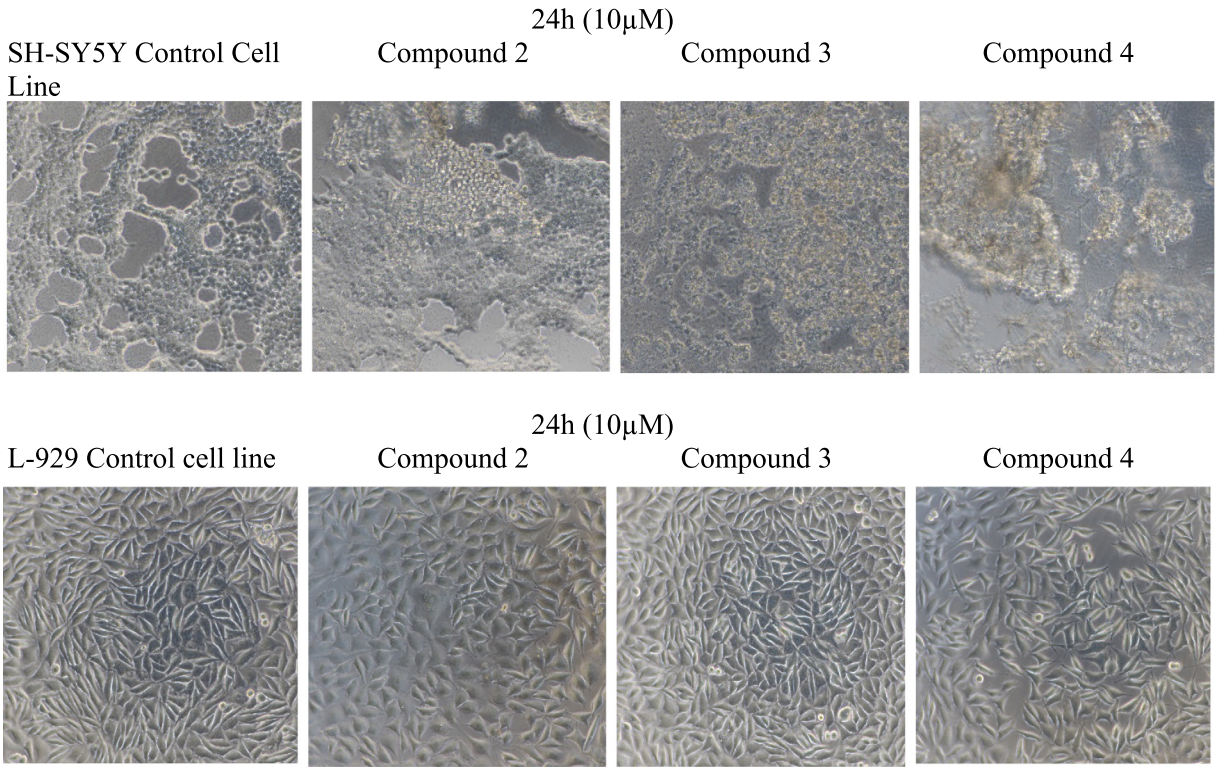

Fig. 8. Morphological changes of SH-SY5Y and L-929 cells after 24 h of incubation with concentrations (10 μM) of Compound 2, 3 and 4 the results presented are from that were carried out and photographed microscopically.

Table 2
The calculated quantum chemical parameters of molecules.

	E_{HOMO}	E_{LUMO}	I	A	ΔE	η	Σ	χ	pi	ω	ε	dipol	Energy
B3LYP/3–21 g LEVEL													
2	−5.6965	0.5627	5.6965	−0.5627	6.2592	3.1296	0.3195	2.5669	−2.5669	1.0527	0.9500	4.3221	−20448.8890
3	−5.7060	0.5423	5.7060	−0.5423	6.2483	3.1242	0.3201	2.5818	−2.5818	1.0668	0.9374	4.0896	−21479.8236
4	−5.8744	−0.3361	5.8744	0.3361	5.5384	2.7692	0.3611	3.1053	−3.1053	1.7410	0.5744	3.7814	−92141.2881
B3LYP/6–31 g LEVEL													
2	−5.7414	0.4683	5.7414	−0.4683	6.2097	3.1048	0.3221	2.6365	−2.6365	1.1194	0.8933	3.8162	−20555.8081
3	−5.7563	0.4411	5.7563	−0.4411	6.1974	3.0987	0.3227	2.6576	−2.6576	1.1397	0.8775	3.5576	−21592.0350
4	−5.8431	−0.3478	5.8431	0.3478	5.4954	2.7477	0.3639	3.0955	−3.0955	1.7436	0.5735	2.5022	−92525.1419
B3LYP/SDD LEVEL													
2	−5.8445	0.2645	5.8445	−0.2645	6.1090	3.0545	0.3274	2.7900	−2.7900	1.2742	0.7848	3.8895	−20558.0934
3	−5.8374	0.2678	5.8374	−0.2678	6.1052	3.0526	0.3276	2.7848	−2.7848	1.2703	0.7872	3.8230	−21594.3055
4	−5.8513	−0.6939	5.8513	0.6939	5.1574	2.5787	0.3878	3.2726	−3.2726	2.0766	0.4816	2.8820	−22914.7338
HF/3–21 g LEVEL													
2	−8.1529	4.3647	8.1529	−4.3647	12.5176	6.2588	0.1598	1.8941	−1.8941	0.2866	3.4893	3.7056	−20310.3300
3	−8.1556	4.3634	8.1556	−4.3634	12.5190	6.2595	0.1598	1.8961	−1.8961	0.2872	3.4821	3.6190	−21334.7173
4	−8.2693	3.5081	8.2693	−3.5081	11.7775	5.8887	0.1698	2.3806	−2.3806	0.4812	2.0781	3.6674	−91945.1993
HF/6–31 g LEVEL													
2	−8.0571	4.2877	8.0571	−4.2877	12.3448	6.1724	0.1620	1.8847	−1.8847	0.2877	3.4755	3.4580	−20415.3596
3	−8.0590	4.2828	8.0590	−4.2828	12.3418	6.1709	0.1621	1.8881	−1.8881	0.2888	3.4621	3.3178	−21444.9778
4	−8.1052	3.4366	8.1052	−3.4366	11.5418	5.7709	0.1733	2.3343	−2.3343	0.4721	2.1181	2.2213	−92325.3638
HF/SDD LEVEL													
2	−8.1529	3.9669	8.1529	−3.9669	12.1198	6.0599	0.1650	2.0930	−2.0930	0.3614	2.7667	3.6258	−20417.8535
3	−8.1540	3.9669	8.1540	−3.9669	12.1209	6.0604	0.1650	2.0935	−2.0935	0.3616	2.7655	3.5345	−21447.5398
4	−8.1586	2.6670	8.1586	−2.6670	10.8256	5.4128	0.1847	2.7458	−2.7458	0.6964	1.4359	2.4855	−22757.6245
M062X/3–21 g LEVEL													
2	−7.0788	1.5404	7.0788	−1.5404	8.6193	4.3096	0.2320	2.7692	−2.7692	0.8897	1.1240	4.1576	−20439.1755
3	−7.0818	1.5391	7.0818	−1.5391	8.6209	4.3105	0.2320	2.7714	−2.7714	0.8909	1.1224	4.1196	−21469.8483
4	−7.2421	0.6555	7.2421	−0.6555	7.8976	3.9488	0.2532	3.2933	−3.2933	1.3733	0.7282	3.8341	−92132.9277
M062X/6–31 g LEVEL													
2	−7.0952	1.4275	7.0952	−1.4275	8.5227	4.2613	0.2347	2.8338	−2.8338	0.9423	1.0613	3.7682	−20546.3986
3	−7.1104	1.4063	7.1104	−1.4063	8.5167	4.2583	0.2348	2.8520	−2.8520	0.9551	1.0470	3.5450	−21582.3324
4	−7.2271	0.4446	7.2271	−0.4446	7.6718	3.8359	0.2607	3.3912	−3.3912	1.4991	0.6671	3.5889	−92517.4545
M062X/SDD LEVEL													
2	−7.1975	1.2106	7.1975	−1.2106	8.4081	4.2041	0.2379	2.9934	−2.9934	1.0657	0.9384	3.8959	−20549.1467
3	−7.2048	1.2041	7.2048	−1.2041	8.4089	4.2045	0.2378	3.0004	−3.0004	1.0705	0.9341	3.8239	−21585.1834
4	−7.8941	0.2291	7.8941	−0.2291	8.1232	4.0616	0.2462	3.8325	−3.8325	1.8081	0.5531	2.8065	−22904.2942

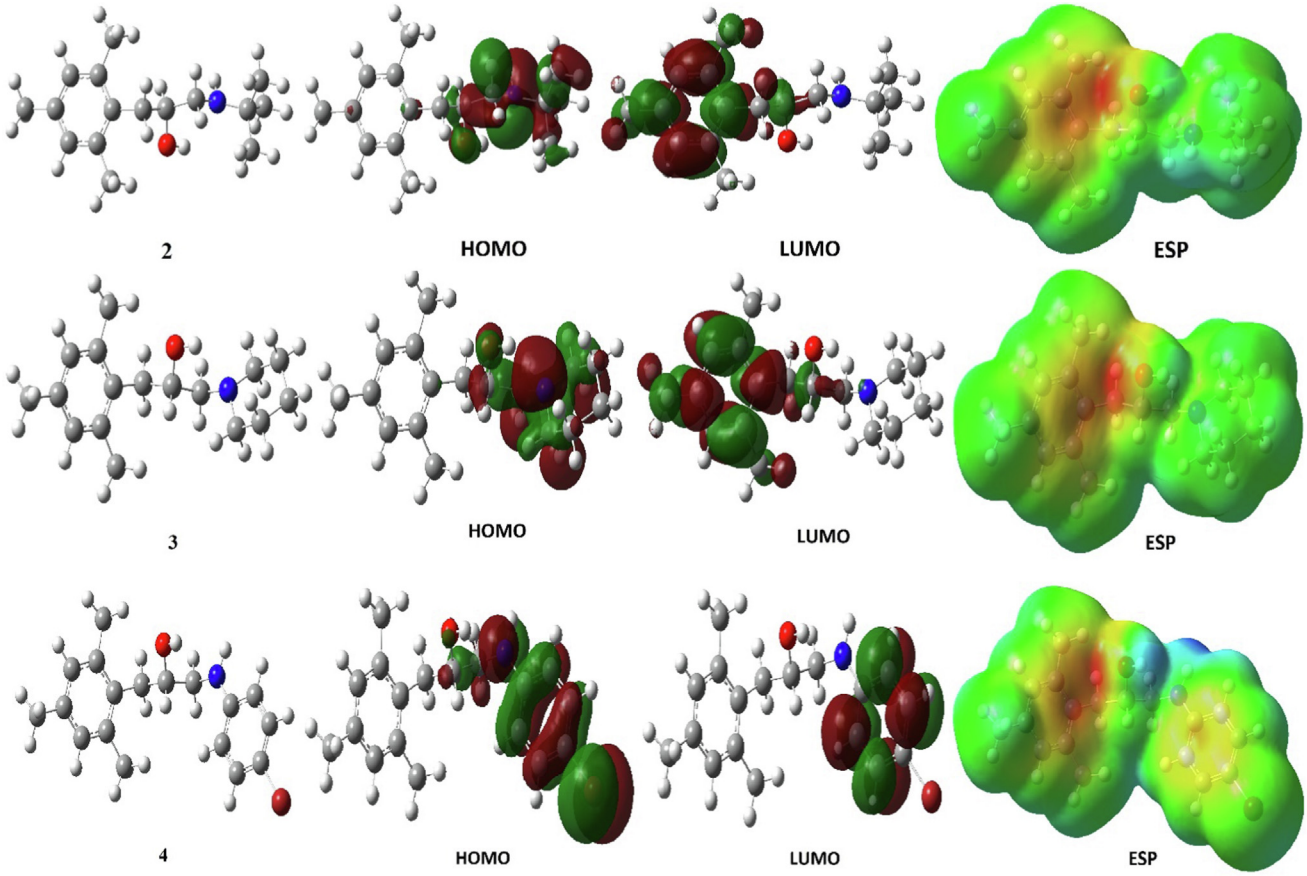

Fig. 9. Representations of optimized structures, HOMO, LUMO, and ESP of compound 2, 3, and 4.

in Fig. S1-S9. In NMR analysis, the chemical shift values of the carbon and hydrogen atoms in the molecule are calculated by the effect of the atoms or atoms around the atoms [51]. In the theoretical calculations made, the chemical shifts values of carbon and hydrogen atoms in the molecule were calculated on a HF/6-31++g basis set. All numerical values obtained as a result of experimental and theoretical operations are given in Tables S1, S2, and S3. Plotted against theoretical values versus experimental values. Calculations of molecules in gas, methanol, DMSO (Dimethyl sulfoxide) phases were made. The theoretical values obtained were plotted against the experimental values in the Fig. S10-S12.

Correlation coefficient values of each curve are found in this graph. In the drawn graph, the correlation coefficient values of the gas phase, methanol phase, and DMSO phase for compound 2 are 0.9984, 0.9983, and 0.9983, respectively. Correlation coefficient values of the gas phase, methanol phase, and DMSO phase, respectively, for compound 3 are 0.9943, 0.9969, and 0.9969, respectively. Finally, for compound 4, the correlation coefficient values of the gas phase, methanol phase, and DMSO phase, respectively, are 0.9968, 0.9975, and 0.9975, respectively. The correlation coefficient values obtained are very close to 1. These correlation coefficient values were generally found to be closer to the experimental values in the methanol and DMSO phases. The high R^2 values of the molecules indicate that the calculated theoretical values are reliable. In the theoretical calculations made, aromatic carbon chemical shift values were found to be between 106.88 and 148.90 [50]. However, chemical shift values of aliphatic carbons were found to be between 20.80 and 70.00 [51]. On the other hand, chemical shift values of aromatic hydrogen atoms were found to be between 6.66 and 6.79 [46].

3.2.2. Ultraviolet and visible light (UV–vis) absorption

Ultraviolet and visible light (UV–vis) absorption is based on the principle of stimulation of electrons in the molecule as a result of the absorption of the light sent to the molecules by the molecule. each molecule is excited by a different wavelength of light [46,48]. With the ultraviolet and visible light (UV–vis) absorption method, it is possible to use the molecules in the process of recognizing molecules as a result of the absorption of rays of different wavelengths. It is also possible to determine the amount of substance from the intensity of the absorbed beam. The molecules studied were gas (ε = 1), chloroform (ε = 4.711), methanol (ε = 32.613), dimethyl sulfoxide (ε = 46.826), water (ε = 78.355), and n methyl formamide-mixture (ε = 181.56). The UV–vis spectrum was obtained in the phases. These spectrum values are calculated on HF/6-31++g basis set. The representations of the experimental and theoretical UV–Vis spectrum values of compound 2–4 are given in Fig. S13-S18.

The most important reason to study so many solvents is to examine how the solvent phase affects the absorbance values. besides, it is to investigate in which solvent the curve similar to the experimental curve will be obtained. When the experimental and theoretical UV–vis spectra of the molecules were examined, it was seen that there were two main peaks. As a result, it has been observed that there are $n \rightarrow n^*$ and $\pi \rightarrow \pi^*$ transitions in molecules.

3.2.3. Infrared spectroscopy

Infrared spectroscopy method is the measurement of the rays sent to the molecule by absorption, emission or reflection by the molecule. Infrared spectroscopy is used like other methods to

Fig. 10. Presentation interactions of afzelin with AChE enzyme.

recognize and study molecules. In the theoretical calculations of the IR spectra of molecules, calculations were made on the basis set HF/6-31++g. Both experimental and theoretical spectra obtained in Figs. S19-S21 are given. In these spectra, the blue colored spectra are the experimental spectrum, the red colored spectra are the theoretical spectrum.

Examining the functional groups, combinations of different substances, and potential changes in the structure of substances is very essential in terms of the structure of the material. FTIR is often used to analyze and describe the structure of a material and to study the interaction of different groups. In this study, FTIR analyzes were performed to observe functional groups. In all Figs. S19–S21, N—H stretching is observed between 3000 and 3400 cm^{-1} [46,48]. In addition, O—H and N—H overlap at the same wavelengths. The C—H stretching appeared between 2921 and 2880 cm^{-1} in Fig. S19. Similarly, Figs. S20 and S21 may overlap with the C—H vibrational bond in the range of 3000–2800 cm^{-1}. Due to the chemical structure of the materials, it can be seen from the figures that there is a C—H bond between 1400 and 600 cm^{-1}. As seen in Figs. S19–S21, it is seen that there is no peak in the 2800–1500 cm^{-1} region in the products formed after the synthesis.

3.2.4. Molecular docking

Molecular docking calculations are performed to compare the biological activities of molecules against biological materials. Many parameters are calculated from the calculations made to compare the activities of molecules against cancer proteins [52,53]. These parameters are used in molecular docking calculations to explain the chemical interactions that occur between molecules and proteins. The most important parameter among these parameters is the docking score. The molecule with the most negative numerical value of this parameter is considered to have higher activity than the other molecular. The most important factor determining the numerical value of the molecular docking score parameter is the chemical interaction. The interactions between cancer proteins, which are composed of many proteins, and molecules, determine the numerical value of the docking score parameter [54]. As the interactions between molecules and proteins increase, the numerical value of the docking score parameter becomes more negative

Fig. 11. Presentation interactions of afzelin with α-Gly enzyme.

Table 3
Numerical values of the docking parameters of molecule against enzymes.

AChE	2	3	4
Docking Score	−7.51	−6.81	−7.06
Glide ligand efficiency	−0.42	−0.36	−0.34
Glide hbond	−0.11	0.00	−0.20
Glide evdw	−24.96	−25.98	−35.82
Glide ecoul	−11.13	−11.44	−4.27
Glide emodel	−58.58	−57.94	−55.05
Glide energy	−36.09	−37.42	−40.08
Glide einternal	3.26	1.15	3.92
Glide posenum	293	129	76
α-Gly	**2**	**3**	**4**
Docking Score	−4.93	−4.92	−4.20
Glide ligand efficiency	−0.26	−0.26	−0.20
Glide hbond	−0.48	−0.36	−0.30
Glide evdw	−18.31	−21.76	−22.14
Glide ecoul	−12.73	−12.44	−9.56
Glide emodel	−44.83	−49.96	−37.03
Glide energy	−31.04	−34.20	−31.70
Glide einternal	3.02	3.58	9.08
Glide posenum	56	72	362

[55]. Therefore, the biological activity of the molecule is higher than other molecules. These interactions have many interactions such as hydrogen bonds, polar and hydrophobic interactions, π-π and halogen [56–59]. These interactions are shown in Figs. 10 and 11.

Many parameters are derived from molecular docking calculations, which are used to describe the chemical interactions between molecules and proteins, are given Table 3. Glide ligand efficiency parameter shows the efficiency of ligand molecules. Glide hbond, Glide evdw, and Glide ecoul parameters are numerical values of chemical interactions of molecules with cancer proteins [57]. The remaining parameters are take numerical data about the exposure between molecules and cancer proteins [58].

The biological activities of the molecules were compared with molecular docking calculations. After this comparison, the properties of molecules to be drugs are examined. ADME/T (Absorption, Distribution, Metabolism, Excretion and Toxicity) analysis was performed to predict the movements of these drug candidate molecules in human metabolism. All calculated parameters of ADME/T are given in Table 4. In this analysis, many movements of molecules in tissues were predicted. As a result of this analysis, it is possible to synthesize more effective drugs by predicting toxicological effects. As a result of the calculated ADME/T analysis, many parameters were found. Among these parameters, many chemical parameters such as molar masses of molecules, dipole moment, hydrogen bonds they give, hydrogen bonds they take, Total solvent accessible surface area, Hydrophobic and Hydrophilic of component of the SASA (solvent accessible surface area), and Predicted polarizability are calculated [59]. Apart from this, many biological parameters such as intestinal-blood barrier, brain-blood barrier, absorption through the skin, and orally usable properties of molecules are calculated [57].

Apart from these, it is the RuleOfFive and RuleOfThree parameters that determine the properties of being a drug. RuleOfFive is known as Lipinski's rule of five. RuleOfFive [60,61] consists of four rules. these rules are mol_MW < 500, QPlogPo/w < 5, donorHB ≤ 5, accptHB ≤ 10. RuleOfThree [62] is known as Jorgensen's rule of three. these three rules are QPlogS > -5.7, QP PCaco > 22 nm/s, #Primary Metabolites < 7.

Table 4
ADME properties of molecule.

	2	3	4	Referance Range
mol_MW	249	261	348	130–725
dipole (D)	3.0	2.7	2.6	1.0–12.5
SASA	555	559	595	300–1000
FOSA	458	469	268	0–750
FISA	29	22	41	7–330
PISA	68	68	208	0–450
WPSA	0	0	78	0–175
volume (A^3)	969	983	1035	500–2000
donorHB	2	1	2	0–6
accptHB	2.7	3.7	2.7	2.0–20.0
glob (Sphere = 1)	0.9	0.9	0.8	0.75–0.95
QPpolrz (A^3)	29.4	30.6	33.4	13.0–70.0
QPlogPC16	8.4	8.2	10.6	4.0–18.0
QPlogPoct	13.2	12.7	15.2	8.0–35.0
QPlogPw	6.0	5.7	7.1	4.0–45.0
QPlogPo/w	3.4	3.3	4.7	−2.0–6.5
QPlogS	−3.0	−3.1	−5.3	−6.5–0.5
CIQPlogS	−2.4	−2.4	−5.8	−6.5–0.5
QPlogHERG	−5.0	−4.9	−5.2	(corcern below −5)
QPPCaco (nm/sec)	1320	1543	4004	*
QPlogBB	0.3	0.5	0.0	−3.0–1.2
QPPMDCK (nm/sec)	739	875	5915	*
QPlogKp	−3.3	−3.3	−1.0	Kp in cm/hr
IP (ev)	9.0	9.0	8.4	7.9–10.5
EA (eV)	−0.5	−0.5	0.1	−0.9–1.7
#metab	6	6	7	1–8
QPlogKhsa	0.4	0.4	0.6	−1.5–1.5
Human Oral Absorption	3	3	3	–
Percent Human Oral Absorption	100	100	100	**
PSA	28	21	30	7–200
RuleOfFive	0	0	0	Maximum is 4
RuleOfThree	0	0	1	Maximum is 3
Jm	0.1	0.1	0.2	–

* <25 is poor and > 500 is great, ** <25% is poor and > 80% is high.

Table 5
The enzyme inhibition results of novel compounds (**2**–**4**) against acetylcholinesterase and α-glucosidase enzymes.

Compounds	IC_{50} (μM)				Ki (μM)	
	AChE	r^2	α-Gly	r^2	AChE	α-Gly
2	63.52	0.9451	6.13	0.9482	54.76 ± 7.73	6.25 ± 0.46
3	75.84	0.9832	4.18	0.9462	71.25 ± 8.22	3.15 ± 0.65
4	92.71	0.9951	0.88	0.9539	90.27 ± 9.66	0.81 ± 0.13
TAC*	125.27	0.9921	–	–	117.48 ± 23.61	–
ACR*	–	–	11.84	0.9391	–	9.44 ± 1.81

* Control compounds.

3.3. Enzymes results

All synthesized compounds against to studied enzymes have inhibitory properties at different μM levels compared to control compounds (tacrine and acarbose) and the results are showed in Table 5. Experimental results show that these compounds have inhibitory potential with IC_{50} values in the range of 63.52–92.71 μM and K_i values 54.76–90.27 μM for AChE. As is clear from Table 1, compound 2 has higher inhibitory potential against AChE (IC_{50}: 63.52 μM; K_i: 54.76 ± 7.73 μM), compared by tacrine compound (IC_{50}: 125.27 μM, K_i: 117.48 ± 23.61). The alpha glucosidase inhibitory activities of these compounds observed with IC_{50} values in the range of 0.88–6.13 and K_i values 0.81–6.25 μM. Molecules with the most inhibitory properties was compound 3 and 4 was more inhibitory potent (IC_{50}: 0.88 μM; K_i: 0.81 μM and IC_{50}: 4.18 μM; K_i: 3.15), while compound 2 have lower inhibitory potential.

Alpha-glucosidase inhibitors (Miglitol, acarbose, voglibose) are extensively used in the therapy of patients with type 2 diabetes. Alpha-glucosidase inhibitors delay the absorption of carbohydrate molecules from the small intestine and thus have a lowering effect on postprandial blood glucose and insulin levels [63,64]. Cholinesterase inhibitors are a group of medicines that block the normal breakdown of acetylcholine. For example, acetylcholine (ACh) is released by motor neurons to activate muscles; ACh also has an key role in attention, arousal, memory, learning, and motivation [65,66].

4. Conclusion

Both chemical and biological activities of molecules were compared with theoretical calculations. It was observed that the activity of compound 2 was higher than the other molecules. For the characterization of the molecules, both experimental and theoretical spectra were compared. It was seen that the obtained theoretical and experimental spectra were in great agreement with each other. Biological activities of molecules against the enzyme were compared with molecular docking calculations. According to the findings, the cytotoxic activity of the compounds was found to be higher in cancer cell line than healthy cell line. As a result, it was concluded that synthesized compounds could be candidates for use in cancer treatment with supportive studies.

CRediT authorship contribution statement

Ali N. Khalilov: Investigation, Writing – original draft, Writing – review & editing. **Burak Tüzün:** Software, Investigation, Writing – original draft, Writing – review & editing. **Parham Taslimi:** Investigation, Writing – original draft, Writing – review & editing. **Ayca Tas:** Investigation. **Zuhal Tuncbilek:** Investigation. **Neşe keklikçioğlu:** Investigation.

Declaration of Competing Interest

The authors declare that they have no known competing financial interests or personal relationships that could have appeared to influence the work reported in this paper.

Acknowledgments

This work is supported by the Baku State University and Scientific Research Project Fund of Sivas Cumhuriyet University under the project number RGD-020. This research was made possible by TUBITAK ULAKBIM, High Performance and Grid Computing Center (TR-Grid e-Infrastructure).

Appendix A. Supplementary material

Supplementary data to this article can be found online at https://doi.org/10.1016/j.molliq.2021.117761.

References

[1] H.-S. Lee, S.H. Kang, Synthesis of physiologically potent β-amino alcohols, Synlett (10) (2004) 1673–1685, https://doi.org/10.1055/s-2004-829578.
[2] A. Viswanathan, D. Kute, A. Musa, S. Konda Mani, V. Sipilä, F. Emmert-Streib, F. I. Zubkov, A.V. Gurbanov, O. Yli-Harja, M. Kandhavelu, Meenakshisundaram Kandhavelu. 2-(2-(2,4-dioxopentan-3-ylidene)hydrazineyl)benzonitrile as novel inhibitor of receptor tyrosine kinase and PI3K/AKT/mTOR signaling pathway in glioblastoma, Eur. J. Medi. Chem. 166 (2019) 291–303.
[3] S.J. Kwon, S.Y. Ko, Synthesis of statine employing a general syn-amino alcohol building block, Tetrahedron Lett. 43 (4) (2002) 639–641.
[4] C.U. Ingram, M. Bommer, M.E.B. Smith, P.A. Dalby, J.M. Ward, H.C. Hailes, G.J. Lye, One-pot synthesis of amino-alcohols using a de-novo transketolase and β-alanine: Pyruvate transaminase pathway in Escherichia coli, Biotechnol. Bioeng. 96 (3) (2007) 559–569.
[5] Miguel Quiliano, Adela Mendoza, Kim Y. Fong, Adriana Pabon, Nathan E. Goldfarb, Isabelle Fabing, Ariane Vettorazzi, Adela Lopez, Ben M. de Cerain, Giovanny Garavito Dunn, David W. Wright, Eric Deharo, Silvia Perez-Silanes, Ignacio Aldana, Silvia Galiano, Exploring the scope of new arylamino alcohol derivatives: synthesis, antimalarial evaluation, toxicological studies, and target exploration, Int. J. Parasitol.: Drugs Drug Resist. 6 (3) (2016) 184–198.
[6] A.M. de Almeida, T. Nascimento, B.S. Ferreira, P.P. de Castro, V.L. Silva, C.G. Diniz, M. Le Hyaric, Synthesis and antimicrobial activity of novel amphiphilic aromatic amino alcohols, Bioorg. Med. Chem. Lett. 23 (10) (2013) 2883–2887.
[7] U.V.S. Reddy, M. Chennapuram, C. Seki, E. Kwon, Y. Okuyama, H. Nakano, Catalytic Efficiency of Primary β-Amino Alcohols and Their Derivatives in Organocatalysis, Eur. J. Org. Chem. 2016 (24) (2016) 4124–4143.
[8] C.P. Pradeep, S.K. Das, Coordination and supramolecular aspects of the metal complexes of chiral N-salicyl-β-amino alcohol Schiff base ligands: towards understanding the roles of weak interactions in their catalytic reactions, Coord. Chem. Rev. 257 (11-12) (2013) 1699–1715.
[9] S.C. Bergmeier, The synthesis of vicinal amino alcohols, Tetrahedron 56 (17) (2000) 2561–2576.
[10] D.J. Ager, I. Prakash, D.R. Schaad, 1,2-Amino alcohols and their heterocyclic derivatives as chiral auxiliaries in asymmetric synthesis, Chem. Rev. 96 (2) (1996) 835–876.
[11] P. Gupta, N. Mahajan, Biocatalytic approaches towards stereoselective synthesis of vicinal amino alcohols, New J. Chem. 42 (2018) 12296–12327.
[12] A.M. Magerramov, A.N. Khalilov, M.A. Allahverdiyev, I.G. Mammadov, G.A. Aliyeva, Synthesis of some arylsubstituted 1,2-aminoalcohols on the base of 1-(2',4',6'-trimethyfenyl)-3-chloropropanole, Chemical Problems 1 (2006) 122–126.

[13] T. Mobasheri, E. Rayzan, M. Shabani, M. Hosseini, G. Mahmoodi Chalbatani, N. Rezaei, Neuroblastoma-targeted nanoparticles and novel nanotechnology-based treatment methods, J. Cell. Physiol. 236 (3) (2021) 1751–1775.
[14] J.M. Maris, Recent advances in neuroblastoma, N. Engl. J. Med. 362 (23) (2010) 2202–2211.
[15] V.R. Ganeshan, N.F. Schor, Pharmacologic management of high-risk neuroblastoma in children, Paediatr. Drugs 13 (4) (2011) 245–255.
[16] J.R. Park, A. Eggert, H. Caron, Neuroblastoma: biology, prognosis, and treatment, Hematol. Oncol. Clin. North Am. 24 (1) (2010) 65–86.
[17] B.A. Kurt, G.T. Armstrong, D.K. Cash, M.J. Krasin, E.B. Morris, S.L. Spunt, L.L. Robison, M.M. Hudson, Primary care management of the childhood cancer survivor, J. Pediatrics 152 (4) (2008) 458–466.
[18] K.A. Mazur, Neuroblastoma: what the nurse practitioner should know, J. Am. Acad. Nurse Practit. 22 (5) (2010) 236–245.
[19] M. Hay, D.W. Thomas, J.L. Craighead, C. Economides, J. Rosenthal, Clinical development success rates for investigational drugs, Nat. Biotechnol. 32 (1) (2014) 40–51.
[20] M. Boztas, P. Taslimi, M.A. Yavari, İ. Gülçin, E. Sahin, A. Menzek, Synthesis and biological evaluation of bromophenol derivatives with cyclopropyl moiety: ring opening of cyclopropane with monoester, Bioorg. Chem. 89 (2019) (2019) 103017.
[21] H. Genc Bilgicli, A. Kestane, P. Taslimi, O. Karabay, A. Bytyqi-Damoni, M. Zengin, İ. Gulçin, Novel eugenol bearing oxypropanolamines: synthesis, characterization, antibacterial, antidiabetic, and anticholinergic potentials, Bioorg. Chem. 88 (2019) (2019) 102931.
[22] E. Bursal, A. Aras, Ö. Kılıç, P. Taslimi, A.C. Gören, İ. Gulçin, Phytochemical content, antioxidant activity and enzyme inhibition effect of Salvia eriophora Boiss. & Kotschy against acetylcholinesterase, α-amylase, butyrylcholinesterase and α-glycosidase enzymes, J. Food Biochem. 43 (3) (2019) e12776.
[23] A. Maharramov, R. Kaya, P. Taslimi, M. Kurbanova, A. Sadigova, V. Farzaliyev, A. Sujayev, İ. Gulçin, Synthesis, crystal structure, and biological evaluation of optically active 2-amino-4-aryl-7,7-dimethyl-5-oxo-5,6,7,8-tetrahydro-4h-chromen-3-carbonitriles: antiepileptic, antidiabetic, and anticholinergics potentials, Arch. Pharm. 352 (2) (2019) 1800317, https://doi.org/10.1002/ardp.v352.210.1002/ardp.201800317.
[24] K. Karrouchi, S. Fettach, B. Tüzün, S. Radi, A.I. Alharthi, H.A. Ghabbour, Y. Garcia, Synthesis, crystal structure, DFT, α-glucosidase and α-amylase inhibition and molecular docking studies of (E)-N'-(4-chlorobenzylidene)-5-phenyl-1H-pyrazole-3-carbohydrazide, J. Mol. Struct. 131067 (2021).
[25] M. Rbaa, A. Oubihi, H. Hajji, B. Tüzün, A. Hichar, E.H. Anouar, E. Berdimurodov, M.A. Ajana, A. Zarrouk, B. Lakhrissi, Synthesis, bioinformatics and biological evaluation of novel pyridine based on 8-hydroxyquinoline derivatives as antibacterial agents: DFT, molecular docking and ADME/T studies, J. Mol. Struct. 1244 (2021) 130934, https://doi.org/10.1016/j.molstruc.2021.130934.
[26] R. Dennington, T. Keith, J. Millam, GaussView, Version 6. Semichem Inc., 2016.
[27] M.J. Frisch, G.W. Trucks, H.B. Schlegel, G.E. Scuseria, M.A. Robb, J.R. Cheeseman, G. Scalmani, V. Barone, B. Mennucci, G.A. Petersson, H. Nakatsuji, M. Caricato, X. Li, H.P. Hratchian, A.F. Izmaylov, J. Bloino, G. Zheng, J.L. Sonnenberg, M. Hada, M. Ehara, K. Toyota, R. Fukuda, J. Hasegawa, M. Ishida, T. Nakajima, Y. Honda, O. Kitao, H. Nakai, T. Vreven, J.A. Montgomery, J.E. Peralta, F. Ogliaro, M. Bearpark, J.J. Heyd, E. Brothers, K.N. Kudin, V.N. Staroverov, R. Kobayashi, J. Normand, K. Raghavachari, A. Rendell, J.C. Burant, S.S. Iyengar, J. Tomasi, M. Cossi, N. Rega, J.M. Millam, M. Klene, J.E. Knox, J.B. Cross, V. Bakken, C. Adamo, J. Jaramillo, R. Gomperts, R.E. Stratmann, O. Yazyev, A.J. Austin, R. Cammi, C. Pomelli, J.W. Ochterski, R.L. Martin, K. Morokuma, V.G. Zakrzewski, G.A. Voth, P. Salvador, J.J. Dannenberg, S. Dapprich, A.D. Daniels, O. Farkas, J.B. Foresman, J.V. Ortiz, J. Cioslowski, D.J. Fox, Gaussian 09, Revision D.01, Gaussian Inc., Wallingford CT, 2009.
[28] D. Vautherin, D.M. Brink, Hartree-Fock calculations with Skyrme's interaction. I. Spherical nuclei, Phys. Rev. C 5 (3) (1972) 626–647, https://doi.org/10.1103/PhysRevC.5.626.
[29] A.D. Becke, Density-functional thermochemistry. III. The role of exact exchange, J. Chem. Phys. 98 (7) (1993) 5648–5652, https://doi.org/10.1063/1.464913.
[30] P.J. Stephens, F.J. Devlin, C.F. Chabalowski, M.J. Frisch, Ab initio calculation of vibrational absorption and circular dichroism spectra using density functional force fields, J. Phys. Chem. 98 (45) (1994) 11623–11627, https://doi.org/10.1021/j100096a001.
[31] K.B. Wiberg, Basis set effects on calculated geometries: 6–311++G** vs. aug-cc-pVDZ, J. Comput. Chem. 25 (11) (2004) 1342–1346, https://doi.org/10.1002/(ISSN)1096-987X10.1002/jcc.v25:1110.1002/jcc.20058.
[32] E.G. Hohenstein, S.T. Chill, C.D. Sherrill, Assessment of the performance of the M05–2X and M06–2X exchange-correlation functionals for noncovalent interactions in biomolecules, J. Chem. Theory Comput. 4 (12) (2008) 1996–2000, https://doi.org/10.1021/ct800308k.
[33] A.T. Bilgiçli, H. Genc Bilgicli, C. Hepokur, B. Tüzün, A. Günsel, M. Zengin, M.N. Yarasir, Synthesis of (4R)-2-(3-hydroxyphenyl) thiazolidine-4-carboxylic acid substituted phthalocyanines: anticancer activity on different cancer cell lines and molecular docking studies, Appl. Organomet. Chem. 35 (7) (2021), https://doi.org/10.1002/aoc.v35.710.1002/aoc.6242.
[34] E. Güzel, A. Günsel, B. Tüzün, G.Y. Atmaca, A.T. Bilgiçli, A. Erdoğmuş, M.N. Yarasir, Synthesis of tetra-substituted metallophthalocyanines: Spectral, structural, computational studies and investigation of their photophysical and photochemical properties, Polyhedron 158 (2019) 316–324.
[35] A. Günsel, A. Kobyaoğlu, A.T. Bilgiçli, B. Tüzün, B. Tosun, G. Arabaci, M.N. Yarasir, Novel biologically active metallophthalocyanines as promising antioxidant-antibacterial agents: synthesis, characterization and computational properties, J. Mol. Struct. 1200 (2020) 127127, https://doi.org/10.1016/j.molstruc.2019.127127.
[36] L. Schrodinger, Small-Molecule Drug Discovery Suite 2019-4, 2019.
[37] Schrödinger Release 2019-4: Protein Preparation Wizard; Epik, Schrödinger, LLC, New York, NY, 2016; Impact, Schrödinger, LLC, New York, NY, 2016; Prime, Schrödinger, LLC, New York, NY, 2019.
[38] Schrödinger Release 2019-4: LigPrep, Schrödinger, LLC, New York, NY, 2019.
[39] F.S. Tokalı, P. Taslimi, İ.H. Demircioğlu, K. Şendil, B. Tuzun, İ. Gülçin, Novel phenolic Mannich base derivatives: synthesis, bioactivity, molecular docking, and ADME-Tox Studies, J. Iran. Chem. Soc. (2021) 1–15.
[40] Schrödinger Release 2020-1: QikProp, Schrödinger, LLC, New York, NY, 2020.
[41] G.L. Ellman, K.D. Courtney, V. Andres Jr, R.M. Featherstone, Biochem. Pharm 7 (2) (1961) 88.
[42] Y. Tao, Y. Zhang, Y. Cheng, Y. Wang, Biomed. Chromatogr. 27 (2013) 148.
[43] A. Riccardi, T. Servidei, A. Tornesello, P. Puggioni, S. Mastrangelo, C. Rumi, R. Riccardi, Cytotoxicity of paclitaxel and docetaxel in human neuroblastoma cell lines, Eur. J. Cancer 31 (4) (1995) 494–499.
[44] B. Tüzün, Investigation of pyrazoly derivatives schiff base ligands and their metal complexes used as anti-cancer drug, Spectrochim. Acta Part A Mol. Biomol. Spectrosc. 227 (2020) 117663.
[45] A. Günsel, A.T. Bilgiçli, H. Pişkin, B. Tüzün, M.N. Yarasir, B. Gündüz, Synthesis of non-peripherally tetra-substituted copper (ii) phthalocyanines: characterization, optical and surface properties, fabrication and photo-electrical properties of a photosensitive diode, Dalton Trans. 48 (39) (2019) 14839–14852.
[46] Hayriye Genc Bilgicli, Parham Taslimi, Busra Akyuz, Burak Tuzun, İlhami Gulcin, Synthesis, characterization, biological evaluation, and molecular docking studies of some piperonyl-based 4-thiazolidinone derivatives, Arch. Pharm. 353 (1) (2020) 1900304, https://doi.org/10.1002/ardp.v353.110.1002/ardp.201900304.
[47] L.K. Ojha, B. Tüzün, J. Bhawsar, Experimental and theoretical study of effect of Allium sativum extracts as corrosion inhibitor on mild steel in 1 M HCl medium, J. Bio-and tribo-corrosion 6 (2) (2020) 1–10.
[48] A.T. Bilgicli, H.G. Bilgiçli, A. Günsel, H. Pişkin, B. Tüzün, M.N. Yarasir, M. Zengin, The new ball-type zinc phthalocyanine with SS bridge; Synthesis, computational and photophysicochemical properties, J. Photochem. Photobiol., A 389 (2020) 112287.
[49] Armağan Günsel, Ahmet T. Bilgiçli, Hasan Pişkin, Burak Tüzün, Nagihan Çaylak Delibaş, M. Nilüfer Yarasir, Bayram Gündüz, Comparison of spectroscopic, electronic, theoretical, optical and surface morphological properties of functional manganese (III) phthalocyanine compounds for various conditions, J. Mol. Struct. 1193 (2019) 247–264.
[50] A. Günsel, A.T. Bilgiçli, B. Tüzün, H. Pişkin, M.N. Yarasir, B. Gündüz, Optoelectronic parameters of peripherally tetra-substituted copper (ii) phthalocyanines and fabrication of a photoconductive diode for various conditions, New J. Chem. 44 (2) (2020) 369–380.
[51] Hayriye Genç Bilgiçli, Ahmet T. Bilgiçli, Armağan Günsel, Burak Tüzün, Derya Ergön, M. Nilüfer Yarasir, Mustafa Zengin, Turn-on fluorescent probe for Zn2+ ions based on thiazolidine derivative, Appl. Organomet. Chem. 34 (6) (2020), https://doi.org/10.1002/aoc.v34.610.1002/aoc.5624.
[52] A. Aktaş, B. Tüzün, R. Aslan, K. Sayin, H. Ataseven, New anti-viral drugs for the treatment of COVID-19 instead of favipiravir, J. Biomol. Struct. Dyn. (2020) 1–11.
[53] A. Aktaş, B. Tüzün, H.A. Taşkın Kafa, K. Sayin, H. Ataseven, clarification of interaction mechanism of arbidol with covid-19 and investigation of the inhibition activity analogues against covid-19, Bratislava Med. J. 121 (10) (2020) 705–711.
[54] M.A. Gedikli, B. Tuzun, A. Aktas, K. Sayin, H. Ataseven, Are clarithromycin, azithromycin and their analogues effective in the treatment of COVID19?, Bratislava Med J. 122 (2) (2021) 101–110, https://doi.org/10.4149/BLL_2021_015.
[55] E. Çetiner, K. Sayin, B. Tüzün, H. Ataseven, Could Boron-Containing Compounds (BCCs) be effective against SARS-CoV-2 as Anti-Viral Agent?, Bratislava Med J. 122 (4) (2021) 263–269, https://doi.org/10.4149/BLL_2021_44.
[56] M.A. Gedikli, B. Tuzun, K. Sayin, H. Ataseven, Determination of inhibitor activity of drugs against the COVID-19, Bratislava Med. J. 122 (7) (2021) 497–506.
[57] B. Tüzün, T. Nasibova, E. Garaev, K. Sayın, H. Ataseven, Could alkaloids be effective in the treatment of COVID-19?, Bratislava Med J. 122 (9) (2021), https://doi.org/10.4149/BLL_2021_108.
[58] H. Ataseven, K. Sayin, B. Tüzün, M.A. Gedikli, Could boron compounds be effective against SARS-CoV-2?, Bratislava Med J. 122 (10) (2021) 753–758, https://doi.org/10.4149/BLL_2021_121.
[59] Alireza Poustforoosh, Hassan Hashemipour, Burak Tüzün, Abbas Pardakhty, Mehrnaz Mehrabani, Mohammad Hadi Nematollahi, Evaluation of potential anti-RNA-dependent RNA polymerase (RdRP) drugs against the newly emerged model of COVID-19 RdRP using computational methods, Biophys. Chem. 272 (2021) 106564, https://doi.org/10.1016/j.bpc.2021.106564.
[60] Christopher A. Lipinski, Lead-and drug-like compounds: the rule-of-five revolution, Drug Discov. Today: Technol. 1 (4) (2004) 337–341.
[61] Christopher A. Lipinski, Franco Lombardo, Beryl W. Dominy, Paul J. Feeney, Experimental and computational approaches to estimate solubility and

permeability in drug discovery and development settings, Adv. Drug Deliv. Rev. 23 (1-3) (1997) 3–25.
[62] William L. Jorgensen, Erin M. Duffy, Prediction of drug solubility from structure, Adv. Drug Deliv. Rev. 54 (3) (2002) 355–366.
[63] Kaan Kucukoglu, Halise Inci Gul, Parham Taslimi, Ilhami Gulcin, Claudiu T. Supuran, Investigation of inhibitory properties of some hydrazone compounds on hCA I, hCA II and AChE enzymes, Bioorg. Chem. 86 (2019) 316–321.
[64] Cetin Bayrak, Parham Taslimi, Halide Sedef Karaman, Ilhami Gulcin, Abdullah Menzek, The first synthesis, carbonic anhydrase inhibition and anticholinergic activities of some bromophenol derivatives with S including natural products, Bioorg. Chem. 85 (2019) 128–139.
[65] Yeliz Demir, Parham Taslimi, Muhammet Serhat Ozaslan, Necla Oztaskin, Yasin Çetinkaya, İlhami Gulçin, Şükrü Beydemir, Suleyman Goksu, Antidiabetic potential. In vitro inhibition effects of bromophenol and diarylmethanones derivatives on metabolic enzymes, Arch. Pharm. 351 (12) (2018) 1800263, https://doi.org/10.1002/ardp.v351.1210.1002/ardp.201800263.
[66] M. Huseynova, A. Medjidov, P. Taslimi, M. Aliyeva, Synthesis, characterization, crystal structure of the coordination polymer Zn(II) with thiosemicarbazone of glyoxalic acid and their inhibitory properties against some metabolic enzymes, Bioorg. Chem. 2019 (83) (2019) 55–62i.